Green Chemistry

PAPER

View Article Online
View Journal

Cite this: DOI: 10.1039/c5gc02228b

Synthesis of 1,6-hexanediol from HMF over double-layered catalysts of Pd/SiO_2 + $Ir–ReO_x/SiO_2$ in a fixed-bed reactor†

Bin Xiao,[a] Mingyuan Zheng,*[a] Xinsheng Li,[a,b] Jifeng Pang,[a] Ruiyan Sun,[a,b] Hua Wang,[a] Xiaoli Pang,[a] Aiqin Wang,[a] Xiaodong Wang[a] and Tao Zhang*[a]

Received 17th September 2015,
Accepted 27th November 2015

DOI: 10.1039/c5gc02228b

www.rsc.org/greenchem

1,6-Hexanediol (1,6-HDO) was effectively prepared from 5-hydroxymethylfurfural (HMF) over double-layered catalysts of Pd/SiO_2 + $Ir–ReO_x/SiO_2$ in a fixed-bed reactor. Under optimal reaction conditions (373 K, 7.0 MPa H_2, in solvent mixtures of 40% water and 60% tetrahydrofuran (THF)), 57.8% yield of 1,6-HDO was obtained. The double-layered catalysts loaded in double-layered beds showed much superior performance compared to that of a single catalyst of $Pd–Ir–ReO_x/SiO_2$, even when the same amount of active components were used in the catalysts. The reaction solvent significantly affected product distributions, giving a volcano-shape plot for the 1,6-HDO yield as a function of the ratio of water to THF. Brønsted acidic sites were generated on the catalyst in the presence of water which played determining roles in 1,6-HDO formation. A high pressure of H_2 contributed to 1,6-HDO formation by depressing the over-hydrogenolysis of reaction intermediates and products to form hexane and hexanol. The reaction route was proposed for HMF conversion to 1,6-HDO on the basis of conditional experiments.

1. Introduction

Stimulated by ever-increasing concerns over the decline of fossil resources and challenges in the sustainable development of economy, synthesis of high value and bulk materials from renewable feedstock has attracted great interests in the past decade.[1,2] 1,6-Hexanediol (1,6-HDO) is a high-value and important diol with dual hydroxyls at the molecule terminals. This structure makes it an ideal monomer for the synthesis of polymers such as polyester,[3] polyurethane,[4] adhesives[5] and unsaturated polyesters.[6] Compared with widely-used polymers such as polyethylene terephthalate (PET) which is made from ethylene glycol,[7–9] polyesters made from 1,6-HDO possess superior properties in flexibility, caustic resistance and hydrolytic stability thanks to the longer carbon chain of 1,6-HDO.[10] Currently, 1,6-HDO is a petrochemical product obtained through multiple reactions including cyclohexane oxidation, esterification and hydrogenation.[10]

Catalytic conversion of biomass produces a variety of important platform chemicals, some of which are suitable to be used as precursors for the synthesis of renewable monomers.[11–13] 5-Hydroxymethylfurfural (HMF) is a typical versatile platform chemical that can be obtained from sugars, cellulose or lignocellulosic biomass by chemical transformations.[14–18] Besides being used for the synthesis of fuels,[19,20] it is also an important intermediate for production of polymer monomers, such as 2,5-furandicarboxylic acid,[21–23] *para*-xylene,[24,25] and 1,6-HDO.[26–30] Buntara *et al.* employed 2,5-bis(hydroxymethyl)-tetrahydrofuran (DHMTHF), a product of selective hydrogenation of HMF, as feedstock for the synthesis of 1,6-HDO.[26] In the presence of mixed catalysts of Nafion SAC-13 and $Rh\text{-}ReO_x/SiO_2$, 86% yield of 1,6-HDO was obtained after a 20 h reaction at 120 °C. They also investigated the conversion of 1,2,6-hexanetriol (1,2,6-HTO) to 1,6-HDO with different catalysts and proposed reaction pathways.[27] Tuteja *et al.* developed one-pot conversion of HMF to 1,6-HDO over a Pd/ZrP catalyst using formic acid as a hydrogen source, and obtain a 43% yield of 1,6-HDO after a 21 h reaction at 413 K.[28] 2-(Hydroxymethyl)tetrahydropyran was also used as a precursor for 1,6-HDO production.[26,29,30] The catalysts containing hydrogenation sites and acid sites, typically consisting of ReO_x and noble metal Rh or Ir, are found to be effective for the selective catalytic breakage of C–O in the furan ring or to obtain terminal diols from biomass.[26,31,32] All of these studies have accumulated much valuable knowledge and afford guidance for the synthesis of 1,6-HDO from biomass. On the other hand, to date the yield of 1,6-HDO is not very high yet when using HMF as feedstock (*ca.* 40%). The reaction

[a]*Dalian Institute of Chemical Physics, Chinese Academy of Sciences, State Key Laboratory of Catalysis, Zhongshan Road 457, Dalian 116023, China. E-mail: myzheng@dicp.ac.cn, taozhang@dicp.ac.cn; Fax: +86 411 84691570; Tel: +86 411 84379738*

[b]*Graduate University of Chinese Academy of Sciences, Beijing 100049, China*

†Electronic supplementary information (ESI) available. See DOI: 10.1039/c5gc02228b

efficiency of these processes is low, usually needing more than 20 h to reach 100% conversion of feedstock. In addition, the reactions were conducted in batch reactors or multiple steps, the operation of which is inefficient from the point of view of industrial applications.[33] Herein, we studied the transformation of HMF into 1,6-HDO in a fixed-bed reactor. A variety of noble metal–rhenium catalysts were screened, and the effects of reaction conditions on the 1,6-HDO yield were investigated. A high yield of 1,6-HDO was effectively obtained over double-layered catalysts under optimized reaction conditions. The reaction route was proposed based on the conditional experiment results. This work may provide inspiration for developing efficient catalysts and reaction systems for 1,6-HDO synthesis from biomass.

2. Experimental

2.1. Materials

HMF (99%) was provided by Ningbo Institute of Industrial Technology. Standard samples (purity >99%), including DHMTHF, 1,6-HDO, and 1,2,6-hexanetriol (1,2,6-HTO) were purchased from J&K Scientific Ltd. The solvent of tetrahydrofuran (THF) was purchased from Tianjin Kermel Chemical Reagent Co., Ltd. Silica (99%, Qingdao Ocean Chemical Ltd, BET surface area 509 $m^2\ g^{-1}$), activated carbon (99%, Beijing Guanghua-Jingke Activated Carbon Co., Ltd, BET surface area 1203 $m^2\ g^{-1}$), TiO_2 (Degussa, P25), SiO_2–Al_2O_3 (Si/Al = 1 : 7, Sinopharm Chemical Reagent Co., Ltd), HZSM-5 (Si/Al = 50, The Catalyst Plant of Nankai University) and perrhenic acid (99%, Alfa Aesar) were purchased from commercial sources and used without further purification. Al_2O_3 is home-made with a surface area of 250 $m^2\ g^{-1}$.

2.2. Catalyst preparation

Pd catalysts supported on different carriers, including SiO_2, Al_2O_3, active carbon (AC), TiO_2, HZSM-5, SiO_2–Al_2O_3, zirconium phosphate, were prepared by incipient wetness impregnation. Taking Pd/SiO_2 as an example, 3.0 g SiO_2 was impregnated with 5.0 mL solution containing 0.14 mmol $PdCl_2{\cdot}2H_2O$ and then dried at 393 K for 12 h. After calcination at 573 K for 3 h, a 0.6 wt% Pd/SiO_2 catalyst was obtained. The zirconium phosphate support was prepared as described in the literature.[28] Differing from other Pd catalysts calcined in air, the active carbon supported Pd catalyst was calcined under a nitrogen atmosphere.

M–ReO_x/SiO_2 (M = Ir, Pd, Pt, Rh, or Pd–Ir, Pd–Rh) catalysts were prepared by step-wise impregnation. M/SiO_2 was first prepared by incipient wetness impregnation with noble metal salt solutions and dried at 393 K for 12 h. Then, it was re-impregnated with an aqueous solution of perrhenic acid. After drying at 393 K for 12 h and calcination at 573 K for 3 h, M–ReO_x/SiO_2 was obtained. For catalysts using other supports, they were prepared by the same process except for the AC supported catalyst which was calcined under a N_2 atmosphere.

2.3. Catalyst characterization

X-ray photoelectron spectra (XPS) were conducted on an ESCALAB 250 X-ray photoelectron spectrometer with a monochromated Al Kα anode. Before the experiment, the sample was reduced at 573 K in flowing hydrogen for 2 h. All binding energies were calibrated for surface charging by referencing them to the energy of the C 1s peak at 284.5 eV.

The metal loadings of Ir–ReO_x/SiO_2 catalysts before and after 24 h of reaction were determined by an inductively coupled plasma atomic emission spectrometer (ICP-AES) on an IRIS Intrepid II XSP instrument (Thermo Electron Corporation).

The FT-IR spectra of pyridine adsorption on the Ir–ReO_x/SiO_2 catalyst after water vapour treatment were collected on a Bruker Equinox 55 spectrometer equipped with a deuterated triglycine sulphate (DTGS) detector in the transmittance mode. In detail, the Ir–ReO_x/SiO_2 catalyst was pressed into self-supporting wafers and reduced under a H_2 stream (40 mL min^{-1}) at 573 K for 1 h. Then, it was cooled to 373 K and evacuated, followed by the introduction of water vapour (saturated at ambient temperature) for 30 min. After cooling to room temperature and thorough evacuation, pyridine was absorbed until saturation. Finally, the IR cell was evacuated at 423 K and IR spectra of the sample were recorded. For comparison, FT-IR spectra of pyridine adsorption on the Ir–ReO_x/SiO_2 catalyst without water treatment were measured by a similar procedure as mentioned above, except for the absence of the water treatment step.

2.4. Catalytic activity measurement

The catalytic conversion of HMF was conducted in a vertical fixed-bed reactor, which was made from a stainless steel tube with an inner diameter of 5 mm. For evaluation of a single catalyst, 1.0 g catalyst (60–80 mesh) was loaded at the centre of the reactor, and quartz granules (60–80 mesh) were filled from both sides. For evaluation of binary catalysts in the double-layered catalyst bed, 1.0 g Pd/SiO_2 was loaded in the upper layer and 1.0 g of the Re-based catalyst was loaded in the bottom layer (the two layers were separated by a thin layer of quartz wool). Prior to reaction, the catalyst was reduced at 573 K for 2 h in flowing H_2 at a rate of 60 mL min^{-1} under 3 MPa pressure. After the temperature decreased to the reaction temperature, the H_2 pressure was modulated to the desired value with a back pressure valve, and then 1% HMF solution was fed into the reactor with an HPLC pump (Model LC-20A, SHIMADZU Company) at a LHSV of 6 h^{-1} (hourly volume of reactant solution/weight of a single catalyst) in flowing hydrogen at a rate of 60 mL min^{-1}. The product solution was collected in a 100 mL tank under the reaction pressure, and periodically released for analysis. The gas products in H_2 were analysed by *in situ* gas chromatography. Typically, the results at 2 h of reaction were adopted in the present contribution.

2.5. Analysis of product

The gas and liquid products were analysed with Agilent 7890B GC equipped with a Varian CP-WAX58 (FFAP) CB capillary

column and a HP-Plot/Q capillary column, respectively. The concentration of HMF after the reaction was measured with an Agilent HPLC which was equipped with a Biorad Aminex HPX-87H organic acid column and an ultraviolet detector (Agilent G 1314 A, operated at 284 nm). The mobile phase was an aqueous solution of 140 mg L^{-1} H_2SO_4 at a flow rate of 0.5 mL min^{-1} and the temperature of the column was set at 318 K.

3. Results and discussion

3.1. Single catalysts' screening

ReO_x based bimetallic catalysts were reported to be active for breaking the C–O bond in the furan ring and hydrodeoxygenation reactions.[30,34–38] Therefore, we first synthesized a series of Re based bimetallic or tri-metallic catalysts and tested them in the one-step conversion of HMF to 1,6-HDO.

As shown in Table 1 (entries 1–4), different noble metal–ReO_x catalysts afforded remarkably different product distributions. It should be mentioned that the solvent THF was stable in the presence of catalysts studied herein, as evidenced by the overall yield of C4 products (1,4-butanediol, butanol, or butane) which was lower than 0.1% on the basis of THF. The dominant product over Pd–ReO_x/SiO_2(5–5%) was DHMTHF with a high yield of 73.0% but no 1,6-HDO was formed. This suggests that Pd catalysts have high activities toward hydrogenation of the aldehyde group and carbon–carbon double bonds in the furan ring to form DHMTHF.[39,40] However, the catalyst showed a low activity in opening the ring of DHMTHF and did not produce 1,6-HDO. Rh–ReO_x/SiO_2 afforded 6.1% yield of 1,6-HDO. This low value is similar to that reported in the literature, where 7% yield of 1,6-HDO was obtained when using HMF as feedstock.[26] Iridium co-loaded with ReO_x showed the best performance, over which 15.2% yield of 1,6-HDO was obtained at the expense of DHMTHF yield which decreased to 10.9%. Tamura *et al.* reported that Ir–ReO_x/SiO_2 was very effective in the selective hydrogenation of C=O in HMF at room temperature but not in the total hydrogenation of HMF.[41] Apparently, the reaction pathway of HMF conversion over Ir–ReO_x/SiO_2 strongly depended on the reaction temperatures.

To improve the 1,6-HDO yield over the Ir–ReO_x/SiO_2 catalyst, Pd was co-loaded with Ir–ReO_x based on the consideration that Pd might promote the hydrogenation of HMF and facilitate the subsequent reactions. However, the 1,6-HDO yield over Pd–Ir–ReO_x/SiO_2(0.6–5–5) (Table 1, entry 5) turned out to be very similar to that of Ir–ReO_x/SiO_2(5–5) (14.6% *vs.* 15.2%), and gave a significant amount of 1,2,6-HTO (30.4% yield). Increasing the Pd loading to 5% led to a slight improvement in the 1,6-HDO yield to 19.2%, which was accompanied by a notable increase in the by-product of 1,5-HDO (entry 6). These results suggest that Pd, Ir, and ReO_x could be used as effective active components for the 1,6-HDO preparation from HMF, but the product selectivity over them needs to be improved through rational design of catalysts and optimization of reaction conditions.

In addition, it was found that catalyst supports affected the product selectivity significantly. Differing from SiO_2 supported catalysts, active carbon supported Ir–ReO_x did not produce 1,6-HDO (Table 1, entry 7) but gave 36% yield of 2-hexanol and many unknown products which were undetectable by GC or HPLC analysis. ZrP and Al_2O_3 supported catalysts did not give a high yield of 1,6-HDO either. Since the SiO_2 supported catalysts showed the best performance for HMF conversion to 1,6-HDO, they were further studied in the following sections.

3.2. Screening of catalysts in a double-layered catalyst bed

Since using a single catalyst met with great challenges in effectively coupling the multiple reactions of HMF conversion to 1,6-HDO, we further employed binary catalysts and loaded them in double layers to improve the selectivity of 1,6-HDO. The catalyst in the upper layer would primarily take charge of hydrogenation of HMF, and the catalyst in the bottom layer fulfills the function of subsequent hydrogenolysis of the furan ring to 1,6-HDO. It was reported that the Pd based catalyst

Table 1 Product yields in HMF hydrogenolysis over different catalysts[a]

Entry	Catalysts	1,6-HDO/%	2,5-HDO/%	1,5-HDO/%	Hexane/%	1-Hexanol/%	DHMTHF/%	MHMTHF/%	1,2,6-HTO/%
1	Pd–ReO_x/SiO_2(5–5)	0	0	0	8.0	0	72.9	8.4	0
2	Pt–ReO_x/SiO_2(5–5)	2.3	0	4.6	23.9	0	32.6	9.1	0
3	Rh–ReO_x/SiO_2(5–5)	6.1	0	0	13.3	0	42.9	0	28.1
4	Ir–ReO_x/SiO_2(5–5)	15.2	0	13.7	18.2	11.7	10.9	0	12.2
5	Pd–Ir–ReO_x/SiO_2(0.6–5–5)	14.6	0	11.5	8.5	0	18.8	6.4	30.4
6	Pd–Ir–ReO_x/SiO_2(5–5–5)	19.1	0	22.0	24.6	4.0	6.8	2.7	0
7	Ir–ReO_x/AC(5–5)[b]	0	0	0	14.2	36.0	0	0	0
8	Ir–ReO_x/ZrP(5–5)[c]	4.8	0	0	13.5	0	0	5.0	0
9	Ir–ReO_x/Al_2O_3(5–5)[d]	0	0	0	14.8	0	42.1	10.5	6.0

[a] Reaction conditions: 373 K, 3 MPa H_2, 1.0 g catalyst loaded in a fixed-bed reactor, mixed solvents of water and THF at a volume ratio of 2 : 3, 1 wt% HMF, LHSV = 6 h^{-1}. HMF conversions were 100% in all experiments. [b] Ir–ReO_x/C(5–5) gave a product of 2-hexanol but not 1-hexanol. [c] Ir–ReO_x/ZrP(5–5) gave a large amount of an unknown precipitate. [d] Ir–ReO_x/Al_2O_3(5–5) gave a product of dihydroxylfurfuran but not DHMTHF. 1,6-HDO, 2,5-HDO, 1,5-HDO, DHMTHF, MHMTHF, and 1,2,6-HTO represent 1,6-hexanediol, 2,5-hexanediol, 1,5-hexanediol, 2,5-bis(hydroxymethyl)-tetrahydrofuran, 5-methyltetrahydrofurfuryl alcohol, and 1,2,6-hexanetriol, respectively.

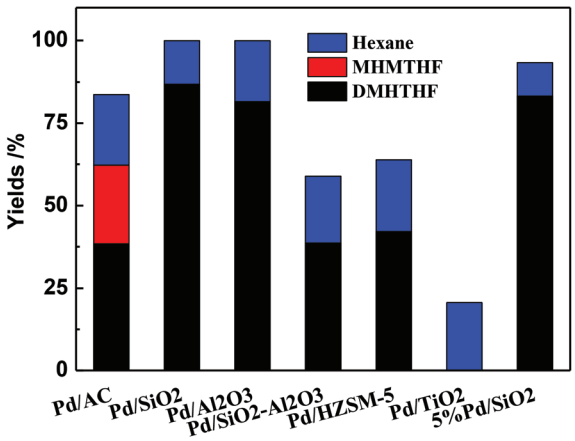

Fig. 1 Results of HMF hydrogenation over Pd catalysts supported on different carriers, the loadings of palladium in all catalysts were 0.6 wt% except 5% Pd/SiO_2. (HMF conversions were 100% in all experiments; reaction conditions: 373 K, 3 MPa H_2, mixed solvents of water and THF at a volume ratio of 2 : 3, 1 wt% HMF, LHSV = 6 h^{-1}.)

could transform HMF to DHMTHF with high selectivity.[42] Therefore, the Pd catalysts supported on different carriers were first screened for obtaining a high selectivity. As shown in Fig. 1, the Pd/SiO_2(0.6%) catalyst showed the highest selectivity (86%) toward DHMTHF with 13% hexane formation at 373 K. Increasing the palladium loading from 0.6 to 5% did not improve DHMTHF selectivity over Pd/SiO_2. The yield of DHMTHF over Pd/Al_2O_3 was slightly lower than that on Pd/SiO_2. In contrast, over the Pd/AC catalyst, besides the formation of DHMTHF and hexane, 22% yield of MHMTHF was also obtained, which is the hydrodeoxygenation product of DMHTHF. Over acidic carriers of SiO_2–Al_2O_3 and HZSM-5 supported Pd catalysts, the yield of DHMTHF was rather low with a significant loss in carbon balance due to the formation of undetectable products. Pd/TiO_2 afforded the worst performance without any DHMTHF production. Taken all together, the 0.6% Pd/SiO_2 catalyst was the best one for use as an upper-layer catalyst in the following study.

Table 2 lists the results of HMF transformation over different double-layered catalysts in a fixed-bed reactor. Compared to the performance of single catalysts listed in Table 1, the 1,6-HDO yield was significantly improved. Over double-layered catalysts of Pd/SiO_2(0.6) + Ir–ReO_x/SiO_2(5–5), 36.1–46.0% yield of 1,6-HDO was obtained (Table 2, entries 1 and 2) in contrast to 14.6% yield of 1,6-HDO (Table 1, entry 5) over a single catalyst of Pd–Ir–ReO_x/SiO_2(0.6–5–5), even though the same loadings of active components were used in both cases. In addition, the performance of Ir–ReO_x/SiO_2(5–5) is notably superior to that of Rh–Re/SiO_2(5–5) (9.7% yield, Table 2, entry 3), which was reported to be active for 1,6-HDO production from DHMTHF.[26] The inferior performance of Rh–Re/SiO_2 might result from no use of an acidic catalyst such as Nafion SAC-13 in the present study.

The 1,6-HDO yield over Pd/SiO_2(0.6) + Ir–ReO_x/SiO_2 first increased and then levelled off at 46.0% with the ReO_x loading increasing from 0.5 to 5%, accompanied by the decrease of the DHMTHF yield from 11.4 to 1.4% (Table 2, entries 1 and 4–6). This indicates that ReO_x played an important role in selectively catalyzing the ring opening of DHMTHF, which is consistent with the findings in the literature.[26,29–32,38] In addition, ReO_x slightly contributed to hexane formation as evidenced by more hexane being formed with the increase of ReO_x loading.

The support of Ir–Re catalysts had remarkable effects on the product selectivity. Compared to the SiO_2 supported catalyst, Al_2O_3 and active carbon supported Ir–Re catalysts gave much lower yields of 1,6-HDO but more DHMTHF formation. Zirconium phosphate supported palladium catalysts were recently reported to be active for the HMF transformation to 1,6-HDO.[28] However, Ir–ReO_x/ZrP in combination with Pd/SiO_2(0.6) did not produce 1,6-HDO, and the primary products were DHMTHF at a high yield of 73.8% (Table 2, entry 7). This suggests that the activity of the Ir–ReO_x/ZrP catalyst for the ring-opening of tetrahydrofuran is very low. Tuteja *et al.*, proposed that over ZrP supported catalysts, HMF was transformed into 1,6-HDO through six-step reactions and an intermediate of hex-1,3,5-triene-1,6-diol.[28] This mechanism would be quite different from that over Pd/SiO_2(0.6) + Ir–ReO_x/SiO_2 studied herein.

Table 2 Product yields in HMF hydrogenolysis over double-layered catalysts[a]

Entry	Catalysts	1,6-HDO/%	1,5-HDO/%	Hexane/%	1-Hexanol/%	DHMTHF/%	MHMTHF/%
1	Pd/SiO_2(0.6) + Ir–ReO_x/SiO_2(5–5)	46.0	18.1	10.0	24.3	1.4	0
2	Pd/SiO_2(0.6) + Ir–ReO_x/SiO_2(5–5)[b]	36.1	15.0	25.3	16.8	0	
3	Pd/SiO_2(0.6) + Rh–ReO_x/SiO_2(5–5)	9.7	9.8	20.8	0	35.6	0
4	Pd/SiO_2(0.6) + Ir–ReO_x/SiO_2(5–2.5)	46.2	19.4	12.9	17.5	4.7	0
5	Pd/SiO_2(0.6) + Ir–ReO_x/SiO_2(5–1)	39.4	11.7	4.5	8.7	7.3	0
6	Pd/SiO_2(0.6) + Ir–ReO_x/SiO_2(5–0.5)	28.7	10.3	6.3	11.3	11.4	0
7	Pd/SiO_2(0.6) + Ir–ReO_x/ZrP (5–5)	0	0	22.5	0	73.8	7.2
8	Pd/SiO_2(0.6) + Ir–ReO_x/C(5–5)	8.2	8.6	23.6	3.5	35.5	0
9	Pd/SiO_2(0.6) + Ir–ReO_x/Al_2O_3(5–5)	15.9	9.3	15.9	0	30.0	0

[a] Reaction conditions: 373 K, 5 MPa H_2, 1.0 g Pd/SiO_2 loaded in the upper layer and 1.0 g of the Re-based catalyst loaded in the bottom layer, mixed solvents of water and THF at a volume ratio of 2 : 3, 1 wt% HMF, LHSV = 6 h^{-1} based on the amount of a single catalyst. HMF conversions were 100% in all experiments. [b] Pd/SiO_2(0.6) + Ir–ReO_x/SiO_2(5–5) was evaluated under 3 MPa H_2. 1,6-HDO, 1,5-HDO, DHMTHF, and MHMTHF represent 1,6-hexanediol, 1,5-hexanediol, 2,5-bis(hydroxymethyl)-tetrahydrofuran and 5-methyltetrahydrofurfuryl alcohol, respectively.

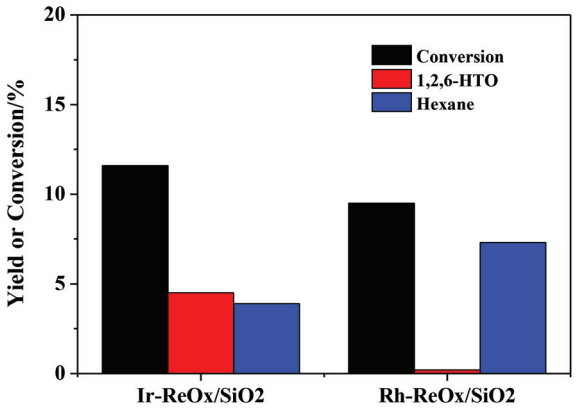

Fig. 2 Results of DHMTHF hydrogenolysis over Ir–ReO_x/SiO_2(5–5) and Rh–ReO_x/SiO_2(5–5) catalysts in a batch reactor, each metal loading on catalysts is 5 wt%. (Reaction conditions: 20 h, 373 K, 5 MPa H_2, 0.15 g catalyst, 20 mL 1% DHMTHF in mixed solvents of water and THF at a volume ratio of 2 : 3.)

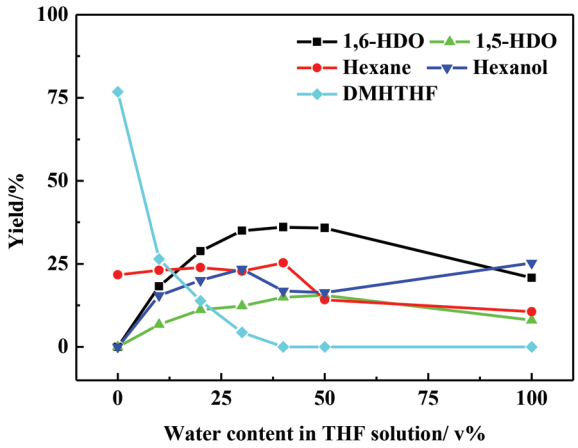

Fig. 3 Effect of water content in the THF solution on the product yields over Pd/SiO_2(0.6%) + Ir–ReO_x/SiO_2(5%–5%) catalysts. (HMF conversions were 100% in all experiments; reaction conditions: 373 K, 3 MPa H_2, 1 wt% HMF, LHSV = 6 h^{-1}.)

It should be noted that the catalysts loaded in the double-layered fixed-bed reactor exhibited remarkably superior performance compared to that in a batch reactor. As shown in Fig. 2, when DHMTHF (the product of HMF hydrogenation over Pd/SiO_2) was used as feedstock in a batch rector in the presence of Ir–ReO_x/SiO_2(5–5) or Rh–ReO_x/SiO_2(5–5), the conversions of DHMTHF were less than 20%. The main product was 1,2,6-HTO and hexane without 1,6-HDO formation even after 20 h of reaction. This suggests that the conversion of DHMTHF was increased by *ca.* 5 folds together with high selectivity to 1,6-HDO in a fixed-bed reactor as compared with that in a batch reactor.

3.3. Effect of the solvent on 1,6-HDO production

The choice of the reactant solvent is an important factor that often remarkably affects the product distribution.[43–45] Two kinds of solvents, *i.e.*, a protic solvent of water and an aprotic solvent of tetrahydrofuran (THF), were used at different mixture ratios for the HMF transformation. As shown in Fig. 3, when pure THF was used as the reaction solvent, the dominant product was DHMTHF (76.8% yield) accompanied by 21.7% yield of hexane, but no 1,6-HDO was formed. In contrast, in a pure water solution, the primary products were 1,6-HDO and hexanol (20.9% and 25.3% yields, respectively), while the yield of DHMTHF decreased nearly to zero. Tuning the ratio of THF to water led to a volcano-shaped curve for the 1,6-HDO yield, which gave a maximum value of 36.1% at 40% water content in the THF solution. A suitable ratio of THF to water benefited HMF conversion to 1,6-HDO. Considering that a pure aqueous solution would be detrimental to the stability of silica supported catalysts due to gradual collapse of the silica support under a hydrothermal environment, a mixed solvent containing 40% water and 60% THF was used as a typical reaction medium in the present study.

As for the reason why the 1,6-HDO selectivity was dramatically different when using THF and water as the solvent, there is still a lack of very clear understanding. For the performance of the upper layer catalyst of Pd/SiO_2 in HMF conversion in different solvents, no big difference was observed with yields of DHMTHF ranging from 89% to 100% (Fig. 4). Therefore, the different selectivity of 1,6-HDO should be primarily ascribed to the effect of the solvent on the catalytic conversion of DHMTHF over the bottom layer Ir–ReO_x/SiO_2 catalyst.

The acidic property of the Ir–ReO_x/SiO_2 catalyst was probed by IR spectroscopy of pyridine adsorption. As shown in Fig. 5, the characteristic peaks occurring at 1450 cm^{-1} and 1544 cm^{-1} belong to Lewis and Brønsted acidic sites, respectively.[46,47] The peak at 1489 cm^{-1} is associated with both Brønsted and Lewis acids.[48] It can be noticed that Brønsted acidic sites were significantly generated on the Ir–ReO_x/SiO_2 catalyst after the

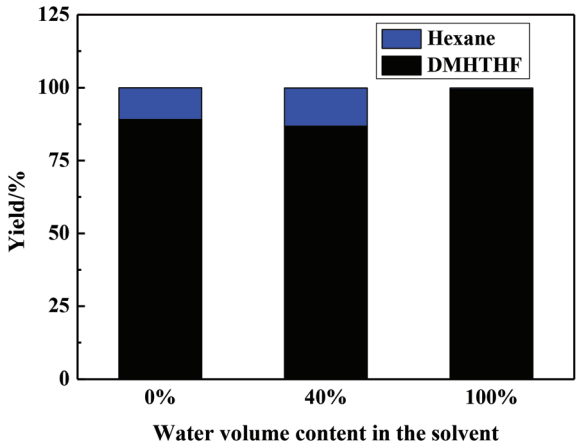

Fig. 4 Effect of water content in the THF solution on HMF conversion to DHMTHF over the upper-layer catalyst of Pd/SiO_2(0.6) without Ir–ReO_x/SiO_2. (HMF conversions were 100% in all experiments; reaction conditions: 373 K, 3 MPa H_2, HMF concentration was 1 wt%, LHSV = 6 h^{-1}.)

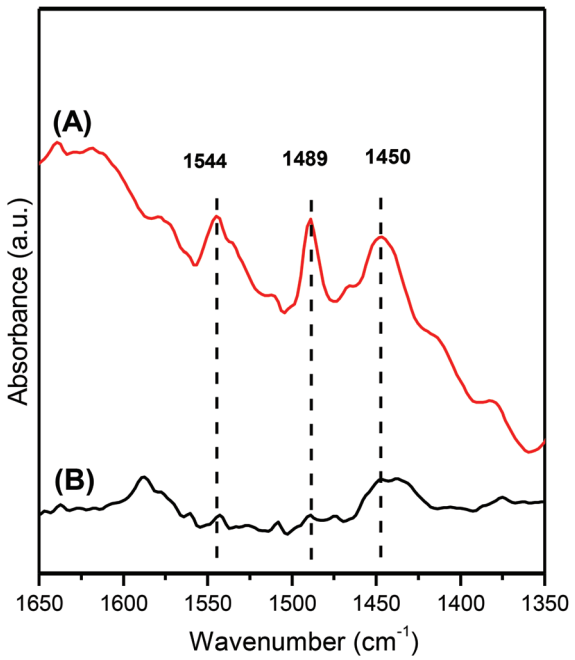

Fig. 5 FT-IR spectra of pyridine adsorbed on the Ir–ReO_x/SiO_2(5–5) catalyst: (A) catalyst treated with water vapour; (B) catalyst without water treatment.

pretreatment with water vapour. The XPS characterization disclosed that a remarkable portion (*ca.* 30%) of Re existed in oxide forms of Re^{4+} on Ir–ReO_x/SiO_2, which could account for the origin of acidic sites (Fig. 6). The STEM and EDX images demonstrated that Ir and Re elements had a very similar distribution on the silica support, suggesting that Ir and Re coexisted closely (ESI Fig. S1†). Chia *et al.* studied the selective hydrogenolysis of secondary C–O bonds for a wide range cyclic ethers and polyols over the ReO_x–Rh/C catalyst.[38] They found that the catalyst realized selective hydrogenolysis of C–O bonds by acid-catalyzed ring-opening and dehydration reactions coupled with metal-catalyzed hydrogenation. The hydroxyl groups on Re atoms associated with metallic Rh are acidic.[38] Tomishige's group studied the Re-modified Ir catalyst and identified that Ir metal particles were modified with ReO_x clusters regardless of whether the catalyst was being used in water or in a *n*-heptane solvent or was freshly reduced under dry conditions.[49–51] Also, they proposed that the protonic acid participated in the catalytic ring opening of tetrahydrofuran.[52] Taken all together, it is rational to conjecture that ReO_x species on Ir–ReO_x/SiO_2 are partially hydrolyzed in the presence of water to produce hydroxyl groups on the surface, which provide Brønsted acidic sites for the catalytic opening of the furan ring of DHMTHF. In contrast, in THF, a non-protonic organic solvent, the amount of hydroxyl groups on the ReO_x surface would be much less, which led to the low activity of DHMTHF conversion (lower than 25%). In addition, as reported by Nakagawa *et al.*, alcohol reactants in an alkane solvent could adsorb on the Ir–ReO_x/SiO_2 catalyst more strongly than that in water.[49] Therefore, in the mixed solvents of THF and water, the abundant amount of Brønsted acidic sites and possibly suitable adsorption strength of reactants could account for the maximum yield of 1,6-HDO in HMF conversion.

3.4. Effect of hydrogen pressure on product distribution

As shown in Fig. 7, the H_2 pressure significantly affected the product distributions. The yield of 1,6-HDO was merely 11.8% but hexane yield reached 76.3% at 0.5 MPa H_2. Increasing H_2 pressure to 7 MPa greatly improved the yield of 1,6-HDO to 57.8% while depressing the hexane yield to 8.6%. The yield of hexanol first increased from zero to 24% and then decreased to 8.2% with H_2 pressure increasing. The high pressure of hydrogen seems to inhibit the further hydrogenolysis of 1,6-HDO to form hexanol and hexane.

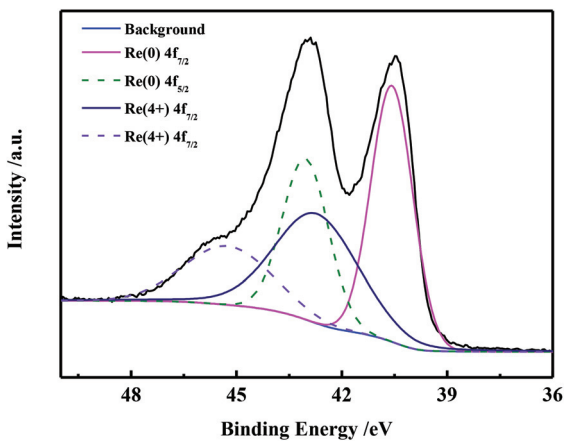

Fig. 6 XPS spectra of the Ir–ReO_x/SiO_2(5%–5%) catalyst.

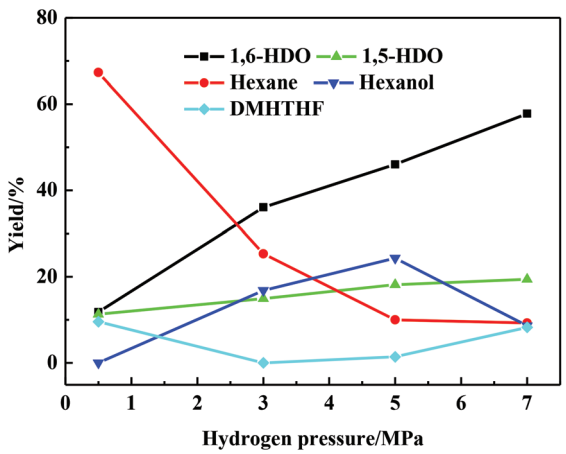

Fig. 7 The product distribution under different hydrogen pressures over Pd/SiO_2(0.6%) + Ir–ReO_x/SiO_2(5%–5%) catalysts. (HMF conversions were 100% in all experiments; reaction conditions: 373 K, mixed solvents of water and THF at a volume ratio of 2 : 3, 1 wt% HMF, LHSV = 6 h^{-1}.)

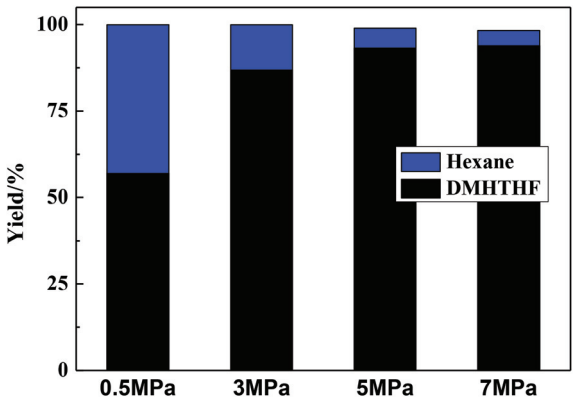

Fig. 8 Effect of hydrogen pressure on the product distribution over the Pd/SiO_2(0.6%) catalyst. (HMF conversions were 100% in all experiments; reaction conditions: 373 K, mixed solvents of water and THF at a volume ratio of 2 : 3, 1 wt% HMF, LHSV = 6 h^{-1}.)

To identify the reasons for the promoting effect of H_2 pressure on 1,6-HDO formation, the catalytic performance of the upper-layer catalyst Pd/SiO_2 was tested. As shown in Fig. 8, the H_2 pressure also imposed notable promoting effects on DHMTHF formation over Pd/SiO_2. With the hydrogen pressure increasing from 0.5 to 7 MPa, the DHMTHF yield was enhanced from 57 to 94% along with a remarkable decrease in the hexane yield. Correlating the yield of DHMTHF in HMF conversion over the upper-layer Pd/SiO_2(0.6%) catalyst (Fig. 8) and the yield of 1,6-HDO over the double-layered catalysts (Fig. 7), the net selectivity of 1,6-HDO in DHMTHF conversion over the bottom-layer $Ir–ReO_x/SiO_2$(5%–5%) catalyst was obtained (Fig. 9). Evidently, H_2 pressure imposed a remarkably positive effect on the selectivity of 1,6-HDO in DHMTHF conversion. Meanwhile, the hexane yield decreased with the increase of H_2 pressure over the bottom layer catalyst.

It was reported that competitive adsorption between hydrogen and reactants on the catalyst surface could depress the hydrogenolysis.[53] With the increase of H_2 pressure, more hydrogen would occupy the metallic active sites and eliminate the coverage of DHMTHF and 1,6-HDO on the upper-layer Pd/SiO_2 catalyst and the bottom-layer $Ir–ReO_x/SiO_2$ catalyst, respectively, which consequently decreased the over-hydrogenolysis of 1,6-HDO to form hexane. In addition, as mentioned in section 3.2, ReO_x sites played roles in hexane formation. Therefore, it can be conjectured that 1,6-HDO should be formed at the interfacial sites between ReO_x and hydrogenation metal sites, which is in agreement with the conclusion reported by Dumesic *et al.*[38] A high pressure of H_2 would contribute to the removal of 1,6-HDO from active sites and decrease the opportunity of the further hydrodeoxygenation of 1,6-HDO to hexane.

3.5. Route for the conversion of HMF to 1,6-HDO

The reaction route of HMF conversion to 1,6-HDO was probed by varying reaction temperatures and conditional experiments. As shown in Fig. 10, the main product was 1,2,6-HTO with 42.4% yield at 333 K, accompanied by 27% yield of DHMTHF and 22% yield of 1,6-HDO. Increasing the temperature led to a continuous decrease in 1,2,6-HTO and DHMTHF yields, while the yield of 1,6-HDO was raised to the highest value of 46% at 373 K. Similarly, as the space velocity of the reaction was increased two and five times, the yield of 1,6-HDO decreased but the yields of 1,2,6-HTO and DHMTHF increased remarkably (ESI Fig. S2†). These results strongly suggested that the 1,6-DHO formation underwent intermediates of DHMTHF and 1,2,6-HTO. In addition, as shown in Fig. 8, over the upper layer Pd/SiO_2 catalyst HMF was converted into DHMTHF at a yield

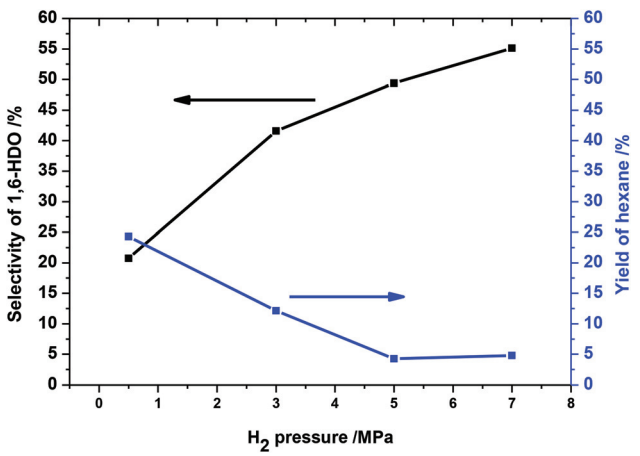

Fig. 9 Net selectivity of 1,6-HDO and net yield of hexane in DHMTHF conversion over the bottom layer catalyst of $Ir–ReO_x/SiO_2$(5%–5%) under different hydrogen pressures. (The net selectivity of 1,6-HDO was obtained by dividing 1,6-HDO yields in Fig. 7 by DHMTHF yields in Fig. 8; the net yield of hexane was obtained by subtracting the yields in Fig. 7 with the yields in Fig. 8.)

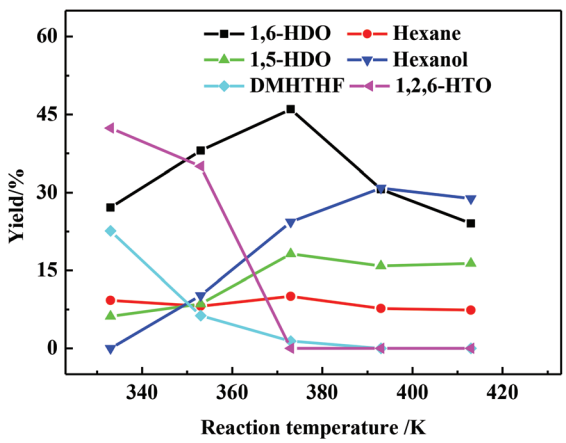

Fig. 10 Effects of reaction temperature on the product distribution for HMF conversion to 1,6-HDO over Pd/SiO_2(0.6%) + $Ir–ReO_x/SiO_2$(5%–5%) catalysts. (HMF conversions were 100% in all experiments; reaction conditions: 5 MPa H_2, mixed solvents of water and THF at a volume ratio of 2 : 3, 1 wt% HMF, LHSV = 6 h^{-1}.)

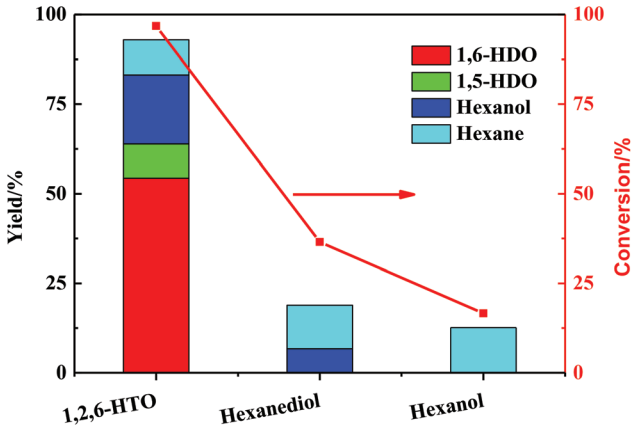

Fig. 11 Results of hydrogenolysis of typical intermediates over the Ir–ReO_x/SiO_2 catalyst. (Reaction conditions: 373 K, 3 MPa H_2, mixed solvents of water and THF (H_2O : THF = 2 : 3/v : v), reactant concentrations were all 1 wt%, LHSV = 6 h^{-1}.)

of 86%. Therefore, it can be inferred that DHMTHF was converted over the bottom layer Ir–ReO_x/SiO_2 catalyst to form 1,2,6-HTO which acted as the precursor of 1,6-HDO. The conditional experiment shows that when 1,2,6-HTO was used as the reaction substrate, 54% yield of 1,6-HDO was obtained, further confirming that 1,2,6-HTO is the precursor of 1,6-HDO (Fig. 11).

The main byproducts of HMF conversion to 1,6-HDO were 1,5-HDO, hexanol and hexane. At 373 K, the ratio of the 1,5-HDO yield to the 1,6-HDO yield was 2/5 in the HMF conversion over the double-layered catalysts Pd/SiO_2(0.6%) + Ir–ReO_x/SiO_2(5%–5%) (Table 2, entry 1). The conditional experiment showed that 1,5-HDO can be produced in 1,2,6-HTO conversion (Fig. 11), but its yield was merely $1/6^{th}$ of that of 1,6-HDO, notably lower than 2/5 in the case of HMF conversion. Therefore, besides being formed from 1,2,6-HTO, nearly half the amount of 1,5-HDO was formed from other precursors, possibly from 5-methyltetrahydrofurfuryl alcohol which is a hydrodeoxygenation product of DHMTHF.

As for the byproduct hexanol, on the one hand it could be derived from 1,6-HDO. As shown in Fig. 11, 6.7% yield of hexanol was obtained when using 1,6-HDO as the reactant. On the other hand, hexanol could also be produced from other polyols, such as 1,5-HDO, according to the fact that the yield of hexanol (16.8%) in HMF conversion is higher than that of hexanol (6.7%) obtained in 1,6-HDO conversion.

Besides, it should be noted that although 1,6-HDO could be hydrodeoxygenated to hexane and hexanol, the conversion of 1,6-HDO was much lower than the conversions of HMF and 1,2,6-HTO. This suggests that 1,6-HDO is more stable than other reaction intermediates over the Ir–ReO_x/SiO_2 catalyst, which is a virtue for obtaining 1,6-HDO at a high yield in HMF conversion.

According to the above analysis, the reaction routes of HMF conversion to 1,6-HDO were proposed and are shown in Scheme 1.

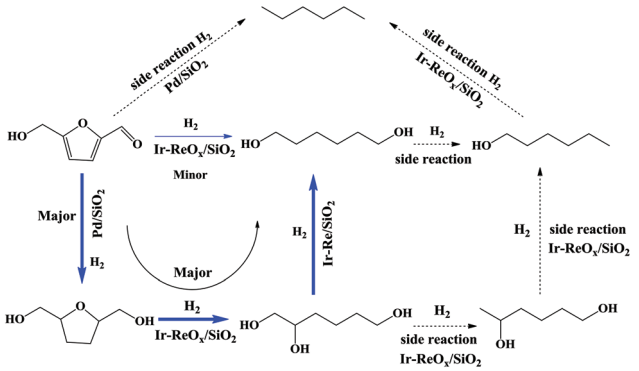

Scheme 1 Reaction routes of HMF conversion to 1,6-HDO over Pd/SiO_2 + Ir–ReO_x/SiO_2 catalysts.

3.6. Catalyst stability

The stability of the optimized catalysts was tested and the results are shown in Fig. 12. The yield of 1,6-HDO was *ca.* 60% at the beginning and was maintained at higher than 50% during 15 h of reaction. After running for 24 h, the 1,6-HDO yield slightly decreased to *ca.* 40%, accompanied by the decrease in yields of hexanol and 1,5-HDO. Conversely, the yield of 1,2,6-HTO significantly increased from zero to 42% after 24 h of reaction. As discussed above, 1,2,6-HTO was the precursor of 1,6-HDO, and its conversion was closely related to the ReO_x species on the catalyst. Elemental analysis showed that loadings of Ir or Pd on the Ir–ReO_x/SiO_2 and Pd/SiO_2 catalysts did not change before and after the reaction. However, the ReO_x loading decreased from 5% to 3% on the spent catalyst. This is consistent with a previous report that Re oxides could leach into the solution in a long running time.[38] In addition, comparing the surface areas and pore size distributions of the catalysts before and after usage, no big differ-

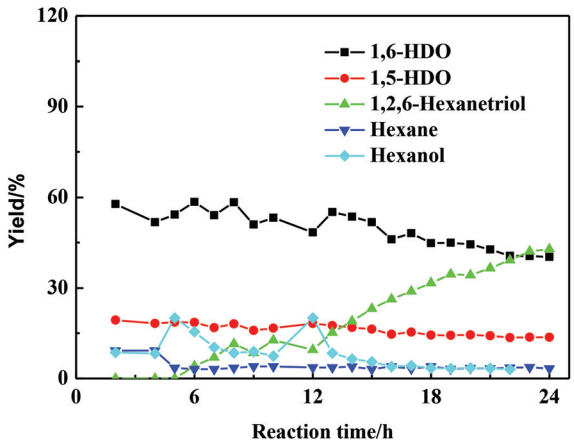

Fig. 12 Results of stability evaluation of Pd/SiO_2(0.6%) + Ir–ReO_x/SiO_2(5%–5%) catalysts. (HMF conversion was 100%; reaction conditions: 373 K, 7 MPa H_2, mixed solvents of water and THF at a volume ratio of 2 : 3, 1 wt% HMF, LHSV = 6 h^{-1}.)

ence was found (*ca.* 400 ± 20 m^2 g^{-1}, 5.6 ± 0.1 nm). It can be concluded that the loss in 1,6-HDO was mainly caused by the leaching of Re during the reaction. Therefore, for the practical application, the stability of the catalyst needed to be further improved by optimizing the preparation method or using more stable active components for the catalyst.

4. Conclusions

In summary, biomass-derived HMF was effectively converted into 1,6-HDO over double-layered catalysts in a fixed-bed reactor. Under optimal reaction conditions of 373 K and 7 MPa H_2, 57.8% yield of 1,6-HDO was obtained over Pd/SiO_2 + $Ir–ReO_x/SiO_2$. The double-layered composite catalyst showed a much superior performance in improving the target product selectivity as compared to that with a single catalyst. The reaction solvent significantly effected 1,6-HDO formation, and mixed solvents of water and THF at a volume ratio of 2 : 3 were the most suitable to afford an enhanced 1,6-HDO yield. A high pressure of H_2 contributed to the formation of 1,6-HDO by depressing the over-hydrogenolysis of reaction intermediates and products to form hexane and hexanol. According to the results of conditional experiments, the reaction route was elucidated, wherein DHMTHF and 1,2,6-HTO were the successive intermediates for the formation of 1,6-HDO. The Pd/SiO_2 + $Ir–ReO_x/SiO_2$ catalysts showed reasonably good stability with the 1,6-HDO yield in the range of 60% to 40% on running for 24 h. The catalyst deactivation was attributed to the gradual leaching of ReO_x during the reaction.

Acknowledgements

This work was supported by the National Nature Science Foundation of China (21376239, 21306191).

Notes and references

1 G. W. Huber, S. Iborra and A. Corma, *Chem. Rev.*, 2006, **106**, 4044–4098.
2 P. Gallezot, *Chem. Soc. Rev.*, 2012, **41**, 1538–1558.
3 C. David, X. Lefèbvre, C. Lefèvre, W. Demarteau and J. M. Loutz, *Prog. Org. Coat.*, 1999, **35**, 45–54.
4 G. Lligadas, J. C. Ronda, M. Galià and V. Cádiz, *Biomacromolecules*, 2010, **11**, 2825–2835.
5 A. B. Foster, P. A. Lovell and M. A. Rabjohns, *Polymer*, 2009, **50**, 1654–1670.
6 N. Kolb and M. A. R. Meier, *Eur. Polym. J.*, 2013, **49**, 843–852.
7 N. Ji, T. Zhang, M. Zheng, A. Wang, H. Wang, X. Wang and J. Chen, *Angew. Chem., Int. Ed.*, 2008, **47**, 8510–8513.
8 Z. Tai, J. Zhang, A. Wang, M. Zheng and T. Zhang, *Chem. Commun.*, 2012, **48**, 7052–7054.
9 B. Xiao, M. Zheng, J. Pang, Y. Jiang, H. Wang, R. Sun, A. Wang, X. Wang and T. Zhang, *Ind. Eng. Chem. Res.*, 2015, **54**, 5862–5869.
10 P. Werle, M. Morawietz, S. Lundmark, K. Sörensen, E. Karvinen and J. Lehtonen, *Ullmann's Encycl. Ind. Chem.*, 2012, **2**, 263.
11 D. Ding, J. Wang, J. Xi, X. Liu, G. Lu and Y. Wang, *Green Chem.*, 2014, **16**, 3846–3853.
12 D. R. Vardon, M. A. Franden, C. W. Johnson, E. M. Karp, M. T. Guarnieri, J. G. Linger, M. J. Salm, T. J. Strathmannb and G. T. Beckham, *Energy Environ. Sci.*, 2015, **8**, 617–628.
13 A. M. Ruppert, K. Weinberg and R. Palkovits, *Angew. Chem., Int. Ed.*, 2012, **51**, 2564–2601.
14 A. Osatiashtiani, A. F. Lee, M. Granollers, D. R. Brown, L. Olivi, G. Morales, J. A. Melero and K. Wilson, *ACS Catal.*, 2015, **5**, 4345–4352.
15 V. Choudhary, S. H. Mushrif, C. Ho, A. Anderko, V. Nikolakis, N. S. Marinkovic, A. I. Frenkel, S. I. Sandler and D. G. Vlachos, *J. Am. Chem. Soc.*, 2013, **135**, 3997–4006.
16 N. Shi, Q. Liu, Q. Zhang, T. Wang and L. Ma, *Green Chem.*, 2013, **15**, 1967–1974.
17 J. M. R. Gallo, D. M. Alonso, M. A. Mellmer and J. A. Dumesic, *Green Chem.*, 2013, **15**, 85–90.
18 R. J. van Putten, J. C. van der Waal, E. de Jong, C. B. Rasrendra, H. J. Heeres and J. G. de Vries, *Chem. Rev.*, 2013, **113**, 1499–1597.
19 Y. Roman-Leshkov, C. J. Barrett, Z. Y. Liu and J. A. Dumesic, *Nature*, 2007, **447**, 982–986.
20 E. R. Sacia, M. H. Deaner, Y. L. Louie and A. T. Bell, *Green Chem.*, 2015, **17**, 2393–2397.
21 B. Saha and M. M. Abu-Omar, *Green Chem.*, 2014, **16**, 24–38.
22 V. Molinari, M. Antonietti and D. Esposito, *Catal. Sci. Technol.*, 2014, **4**, 3626–3630.
23 X. Wan, C. Zhou, J. Chen, W. Deng, Q. Zhang, Y. Yang and Y. Wang, *ACS Catal.*, 2014, **4**, 2175–2185.
24 C. M. Cai, N. Nagane, R. Kumar and C. E. Wyman, *Green Chem.*, 2014, **16**, 3819–3829.
25 Y. Cheng, J. Jae, J. Shi, W. Fan and G. W. Huber, *Angew. Chem., Int. Ed.*, 2012, **51**, 1387–1390.
26 T. Buntara, S. Noel, P. H. Phua, I. Melian-Cabrera, J. G. de Vries and H. J. Heeres, *Angew. Chem., Int. Ed.*, 2011, **50**, 7083–7087.
27 T. Buntara, S. Noel, P. H. Phua, I. Melián-Cabrera, J. G. de Vries and H. J. Heeres, *Top. Catal.*, 2012, **55**, 612–619.
28 J. Tuteja, H. Choudhary, S. Nishimura and K. Ebitani, *ChemSusChem*, 2014, **7**, 96–100.
29 T. Buntara, I. Melián-Cabrera, Q. Tan, J. L. G. Fierro, M. Neurock, J. G. de Vries and H. J. Heeres, *Catal. Today*, 2013, **210**, 106–116.
30 K. Chen, S. Koso, T. Kubota, Y. Nakagawa and K. Tomishige, *ChemCatChem*, 2010, **2**, 547–555.
31 Y. Nakagawa, X. Ning, Y. Amada and K. Tomishige, *Appl. Catal., A*, 2012, **128**, 433–434.
32 Y. Nakagawa, M. Tamura and K. Tomishige, *ACS Catal.*, 2013, **3**, 2655–2668.

33 S. Liu, Y. Amada, M. Tamura, Y. Nakagawa and K. Tomishige, *Catal. Sci. Technol.*, 2014, **4**, 2535–2549.
34 S. Koso, I. Furikado, A. Shimao, T. Miyazawa, K. Kunimori and K. Tomishige, *Chem. Commun.*, 2009, 2035–2037.
35 S. Koso, N. Ueda, Y. Shinmi, K. Okumura, T. Kizuka and K. Tomishige, *J. Catal.*, 2009, **267**, 89–92.
36 S. Liu, Y. Amada, M. Tamura, Y. Nakagawa and K. Tomishige, *Green Chem.*, 2014, **16**, 617–626.
37 Y. Nakagawa, Y. Shinmi, S. Koso and K. Tomishige, *J. Catal.*, 2010, **272**, 191–194.
38 M. Chia, Y. J. Pagan-Torres, D. Hibbitts, Q. Tan, H. N. Pham, A. K. Datye, M. Neurock, R. J. Davis and J. A. Dumesic, *J. Am. Chem. Soc.*, 2011, **133**, 12675–12689.
39 Y. Nakagawa, K. Takada, M. Tamura and K. Tomishige, *ACS Catal.*, 2014, **4**, 2718–2726.
40 J. Chen, R. Liu, Y. Guo, L. Chen and H. Gao, *ACS Catal.*, 2015, **5**, 722–733.
41 M. Tamura, K. Tokonami, Y. Nakagawa and K. Tomishige, *Chem. Commun.*, 2013, **49**, 7034–7036.
42 Y. Nakagawa and K. Tomishige, *Catal. Commun.*, 2010, **12**, 154–156.
43 S. Minakata and M. Komatsu, *Chem. Rev.*, 2009, **109**, 711–724.
44 G. W. Huber, J. N. Chheda, C. J. Barrett and J. A. Dumesic, *Science*, 2005, **308**, 1446–1450.
45 L. R. Merte, G. Peng, R. Bechstein, F. Rieboldt, C. A. Farberow, L. C. Grabow, W. Kudernatsch, S. Wendt, E. Lægsgaard, M. Mavrikakis and F. Besenbacher, *Science*, 2012, **336**, 889–893.
46 M. Stoyanova, U. Rodemerck, U. Bentrup, U. Dingerdissen, D. Linke, R. W. Mayer, H. G. J. Lansink Rotgerink and T. Tacke, *Appl. Catal., A*, 2008, **340**, 242–249.
47 G. Busca, *Phys. Chem. Chem. Phys.*, 1999, **1**, 723–736.
48 W. N. P. van der Graaff, G. Li, B. Mezari, E. A. Pidko and E. J. M. Hensen, *ChemCatChem*, 2015, **7**, 1152–1160.
49 Y. Nakagawa, K. Mori, K. Chen, Y. Amada, M. Tamura and K. Tomishige, *Appl. Catal., A*, 2013, **468**, 418–425.
50 Y. Amada, Y. Shinmi, S. Koso, T. Kubota, Y. Nakagawa and K. Tomishige, *Appl. Catal., B*, 2011, **105**, 117–127.
51 Y. Amada, H. Watanabe, M. Tamura, Y. Nakagawa, K. Okumura and K. Tomishige, *J. Phys. Chem. C*, 2012, **116**, 23503–23514.
52 S. Koso, Y. Nakagawa and K. Tomishige, *J. Catal.*, 2011, **280**, 221–229.
53 J. He, C. Zhao and J. A. Lercher, *J. Am. Chem. Soc.*, 2012, **134**, 20768–20775.

